

Cdc42 Mediates Nucleus Movement and MTOC Polarization in Swiss 3T3 Fibroblasts under Mechanical Shear Stress[□] [▽]

Jerry S.H. Lee,* Melissa I. Chang,* Yiider Tseng,* and Denis Wirtz*^{†‡§}

Departments of *Chemical and Biomolecular Engineering and [†]Materials Science and Engineering and [‡]Graduate Program in Molecular Biophysics, The Johns Hopkins University, Baltimore, MD 21218

Submitted December 19, 2003; Revised November 2, 2004; Accepted November 8, 2004
Monitoring Editor: Jennifer Lippincott-Schwartz

Nucleus movement is essential during nucleus positioning for tissue growth and development in eukaryotic cells. However, molecular regulators of nucleus movement in interphase fibroblasts have yet to be identified. Here, we report that nuclei of Swiss 3T3 fibroblasts undergo enhanced movement when subjected to shear flows. Such movement includes both rotation and translocation and is dependent on microtubule, not F-actin, structure. Through inactivation of Rho GTPases, well-known mediators of cytoskeleton reorganization, we demonstrate that Cdc42, not RhoA or Rac1, controls the extent of nucleus translocation, and more importantly, of nucleus rotation in the cytoplasm. In addition to generating nuclei movement, we find that shear flows also causes repositioning of the MTOC in the direction of flow. This behavior is also controlled by Cdc42 via the Par6/protein kinase C ζ pathway. These results are the first to establish Cdc42 as a molecular regulator of not only shear-induced MTOC polarization in Swiss 3T3 fibroblasts, but also of shear-induced microtubule-dependent nucleus movement. We propose that the movements of MTOC and nucleus are coupled chemically, because they are both regulated by Cdc42 and dependent on microtubule structure, and physically, possibly via Hook/SUN family homologues similar to those found in *Caenorhabditis elegans*.

INTRODUCTION

Nucleus positioning is an essential process in cell development and plays a major role in mating and mitosis in yeast (Hagan and Yanagida, 1997), asymmetric division of zygotes in *Caenorhabditis elegans* (Pellettieri and Seydoux, 2002; Tsou *et al.*, 2003), nucleus organization in interphase murine cells (Abney *et al.*, 1997; Cerda *et al.*, 1999), and motility in human neuronal cells (Morris *et al.*, 1998). To adopt its proper cytoplasmic position, the nucleus must migrate to its destination. The molecular mechanisms that drive such nucleus motion have been investigated in lower eukaryotic cells and have been found to be cytoskeleton dependent (Hagan and Yanagida, 1997; Morris *et al.*, 1998; Reinsch and Gonczy, 1998; Morris, 2000). Early studies on 3T3 fibroblasts have shown that intracellular nucleus movement includes rigid-body motion when these cells are subject to shear stimulus (Tseng *et al.*, 2004) and rigid-body nucleus rotation (NR) when treated with the Golgi-perturbing agent monensin (Paddock and Albrecht-Buehler, 1986). However, the molecular mechanisms that coordinate nucleus motion in fibroblasts remain unknown.

In Swiss 3T3 fibroblasts, both the actin and microtubule (MT) filament networks play a central role in various cellular functions such as maintaining cell shape and adhesion and orchestrating cell migration and division (Hall, 1998; Lane and Allan, 1998; Omelchenko *et al.*, 2002; Small *et al.*, 2002); however, the involvement of F-actin and MT in nucleus movement in those cells remains unexplored. RhoGTPases RhoA, Rac1, and Cdc42 are known major regulators of the organization of the actin and MT cytoskeletons in Swiss 3T3 fibroblasts (Nobes and Hall, 1995; Hall, 1998; Bishop and Hall, 2000; Hollenbeck, 2001; Palazzo *et al.*, 2001; Fukata *et al.*, 2002; Harwood and Braga, 2003; Cerione, 2004; Etienne-Manneville, 2004). RhoGTPases also control the polarization of the microtubule organizing center (MTOC), which is located close to the nucleus in interphase cells (Etienne-Manneville and Hall, 2001; Palazzo *et al.*, 2001; Tzima *et al.*, 2003; Wang *et al.*, 2003; Wojciak-Stothard and Ridley, 2003). However, little is known about the potential regulatory effect of RhoGTPases on the motion of the nucleus and the MTOC in Swiss 3T3 fibroblasts. In particular, it is unclear whether nucleus movement and MTOC positioning are parts of the same signaling pathway.

Here we identify molecular regulators of nucleus movement and MTOC positioning in Swiss 3T3 fibroblasts. We apply mild shear flows onto single interphase cells and investigate the rotation and translocation of the nucleus, as well as the position of the MTOC with respect to the nucleus. Treatments of either actin- or MT-depolymerizing agents demonstrate that the mechanism powering the movements of the nucleus involves mainly the MT network and not the F-actin network. Cell transfections show that both nucleus movement and MTOC repositioning in sheared Swiss 3T3 fibroblasts are controlled by Cdc42, not by RhoA or Rac1. These results suggest that nucleus mo-

Article published online ahead of print in *MBC in Press* on November 17, 2004 (<http://www.molbiolcell.org/cgi/doi/10.1091/mbc.E03-12-0910>).

[□] [▽] The online version of this article contains supplemental material at *MBC Online* (<http://www.molbiolcell.org>).

[§] Corresponding author. E-mail address: wirtz@jhu.edu.

Abbreviations used: MTOC, microtubule organizing center; NR, nuclear rotation; MT, microtubule.

tion and MTOC positioning are intimately coordinated and are downstream events of the same Cdc42 signaling pathway.

MATERIALS AND METHODS

Cell Culture

Swiss 3T3 fibroblasts (ATCC, Rockville, MD) were grown in DMEM (ATCC) containing 10% bovine calf serum (ATCC) in a humidified 5% CO₂/95% air incubator maintained at 37°C. Cells were seeded at a density of 2×10^3 cells/ml on the fibronectin-coated coverslips described below. Seeded cells were allowed to grow for 24 h before use.

Flow Chamber Assay

Thirty-five-millimeter diameter circle coverslips (VWR, Mississauga, ON, Canada) were treated first with 1 M HCl overnight at 55°C, rinsed, and coated with 0.1% poly-L-lysine (Sigma, St. Louis, MO) for 15 min. The coverslips were then coated with bovine plasma fibronectin (Calbiochem, La Jolla, CA) at 20 µg/ml concentration for 1 h. At this concentration, the amount of adsorbed fibronectin on the surface becomes independent of bulk fibronectin concentration (Goldstein and DiMilla, 2002). A parallel-plate flow chamber (Glycotech, Gaithersburg, MD) was placed on top of cell-seeded coverslips using a 0.127-mm thickness gasket with flow width of 2.5 mm. The wall shear stress produced by the flow, τ_w (dyn/cm²), was calculated using the Navier-Stokes equation for Newtonian fluid flow between parallel plates, $\tau_w = 6\mu Q/h^2w$, where μ is the viscosity of the media at 37°C (expressed in Poise), Q is the volumetric flow rate (ml/s), h is channel height (cm), and w is the channel width (cm). The cells were subject to shear flows for 40 min at a wall shear stress value of 9.4 dyn/cm². It has been shown that 3T3 fibroblasts do not detach from similar substrate until the wall shear stress is increased to 50–60 dyn/cm² (Goldstein and DiMilla, 2002), and so our choice of wall shear stress ensured that shear flow was merely used as a mechanical stimulus and would not affect cell adhesion (Tseng *et al.*, 2004).

Drug Treatment

Nocodazole (Sigma) and latrunculin B (LA-B, Sigma) were diluted from the stock using serum-free media. Nocodazole was used at a final concentration of 1 µg/ml. LA-B was used at final concentrations of 80 nM, 160 nM, 315 nM, 630 nM, and 1.6 µM. Cells were incubated with either nocodazole or LA-B for 30 min before shear flow was applied. Nocodazole and LA-B were also placed in shear media to ensure there was no recovery of disrupted microtubule and F-actin structure, respectively.

DNA Constructs

To generate EGFP-tagged constructs, dominant negative forms of RhoGTPases Cdc42 (Cdc42T17N), RhoA (RhoAT19N), and Rac1 (Rac1T17N; Guthrie cDNA Resource Center; www.cdna.org) were individually extracted and amplified using PCR. All three constructs shared a common forward primer (5'-CTCCGC-CCCATTGACGCAAATGG-3'), but distinct reverse primers that included an *Xma*I restriction site: Cdc42T17N (5'-TCCCCCGGGTTAGAATATACAG-CACTTCTTTTG-3'), RhoAT19N (5'-TCCCCCGGGTCTGAGTCAACAAG-3'), and Rac1T17N (5'-TCCCCCGGGCTCGAGTTACAACAG-3'). PCR products were digested with *Hind*III and *Xma*I and cloned into the pEGFP-C1 vector (BD Biosciences, San Diego, CA). Protein kinase C (PKC) ζ and Par6B constructs were generous gifts from Dr. Ian Macara (Bandyopadhyay *et al.*, 1997; Joberty *et al.*, 2000). The inactive form of Par6B, Δ Nt Par6B, was generated by sufficient deletion of the N-terminus semi-CRIB domain, thus inactivating its ability to bind to both GDP and GTP-bound GTPases (Joberty *et al.*, 2000). DN PKC ζ is a kinase inactive form of PKC ζ generated by point mutation at Lys²⁸¹ to Trp in the catalytic site (Bandyopadhyay *et al.*, 1999).

Cell Transfections

Transfections were conducted using Lipofectamine Plus kit (Invitrogen, Carlsbad, CA). For RhoGTPase constructs, 2.5 µg plasmids, 4 µl Lipofectamine Plus, and 5 µl Lipofectamine were diluted in 2 ml serum-free media. For the other plasmids (WT PKC ζ , DN PKC ζ , WT Par6B, Δ Nt Par6B), a combination of 2.25 µg of selected plasmid and 0.25 µg of pEGFP-C1 was used as described previously (Tzima *et al.*, 2003). Cells were incubated with the plasmids for 3 h and then washed three times with serum media. Fibroblasts were then allowed 24 h to overexpress these proteins before use.

Morphometric and Dynamic Parameters Describing Nucleus Motion in Cells Under Flow Shear Stress

Live-cell microscopy was conducted in an incubator chamber surrounding the microscope that kept a humidified environment at 37°C and 5% CO₂/95% air condition (Tseng *et al.*, 2004). Flow media consisted of DMEM supplemented with 10% BCS and 25 mM HEPES buffer solution (Invitrogen). For drug-treated cells, the flow media also contained the drug at indicated con-

centrations. Cells were subjected to shear flow stresses of 9.4 dyn/cm² for 40 min, and phase contrast images were taken at 100× magnification every minute. Images were collected using a CCD camera (Hamamatsu, Bridgewater, NJ) mounted on a Nikon TE300 microscope (Nikon, Garden City, NY) and analyzed using Metamorph (Universal Imaging, West Chester, PA). Postacquisition, each frame was compared with the previous one and aligned to ensure that no ghost movement of the stage was reported. Regions were traced around the nucleus and nucleoli at each time frame and using the analysis software, we obtained centroid positions as well as the morphometric value σ and the equivalent radius of the nucleus. To calculate the equivalent radius, the analysis software first found the area of the region traced around the nucleus and then calculated the radius of a circle with equivalent area. Translocation of the nucleus within the cytoplasm, δ , was measured by tracking the displacements of the nucleus centroid, which were normalized at each time point by the measured equivalent radius of the nucleus so as to allow for comparison between cells. λ values were calculated as the interdistances between the centroid position of the nucleus and the centroid position of each nucleolus of each cell in each frame. Both σ and λ were normalized with their respective initial values, σ_0 and λ_0 . The centroid positions of the nucleoli also defined the endpoints of a vector pointing away from the centroid of the nucleus toward the centroid of the nucleoli in order to calculate the rotation of each nucleolus-cell center pair in the cell. Each vector in each frame was compared with its initial value ($t = 0$ min) and the angle of rotation was found by using the dot product: $\cos \theta = a \cdot b / |a| \cdot |b|$. For each condition, morphometric measurements were conducted 3–5 times.

Shear-induced Cell Polarization Assay

To assess the polarization of cells we used a standard scoring assay based on the position of the MTOC with respect to the nucleus (Tzima *et al.*, 2002). Cells were subject to shear flow stresses of 9.4 dyn/cm² for 40 min and then fixed with 2% paraformaldehyde for 1 h. Cells were then permeabilized with 0.1% Triton X-100 for 10 min. BCS, 10%, in phosphate-buffered saline was used to block nonspecific binding for 20 min and the cells were then treated with α -tubulin monoclonal antibody (Oncogene, Boston, MA) at 1:20 dilution. Next, cells were incubated in Alexa-568 goat anti-mouse antibody at 1:40 and 300 nM of DAPI for 1 h (Molecular Probes, Eugene, OR) to visualize microtubules and nuclear DNA, respectively. MTOC location was determined by first overlaying Alexa-568 and DAPI fluorescence images using Metamorph (Universal Imaging). The nucleus was then divided into two regions—one in the direction and one in the opposing direction of flow—to determine the location of the MTOC in relation to the division (see Figure 5A). F-actin was stained using Alexa-488 phalloidin (Molecular Probes).

RESULTS

Rotation and Translocation of the Nucleus

The nucleus of Swiss 3T3 fibroblast exhibits enhanced motion when treated with either monensin (Paddock and Albrecht-Buehler, 1986) or mechanical shear flow (Tseng *et al.*, 2004). Using time-lapse phase contrast microscopy and a parallel-plate flow chamber, we documented nucleus motion within the cytoplasm of a single sheared Swiss 3T3 fibroblast (Figure 1A and Supplementary Movie 1). Application of shear flow caused minor displacement of the cells, but induced large excursions of the nucleus with respect to the rest of the cell (Figure 1B). To quantify the motion and shape of the nucleus, the following dynamic and morphometric parameters were monitored. First, we measured the translocation of the nucleus within the cytoplasm, δ , normalized by the equivalent radius of the nucleus (Figure 1C and *Materials and Methods*). Second, changes in the interdistances, λ , between the centroids of the nucleus and each nucleolus were measured as described previously (Tseng *et al.*, 2004) to monitor changes in intranuclear integrity (Figure 1D). Third, changes in the shape factor of the nucleus, σ , were computed to measure possible deformations in the nuclear envelope (Figure 1D). Finally, the degree of nuclear rotation (NR), θ , was quantified by monitoring the centroid displacements of each nucleolus with respect to the centroid position of the nucleus (Figure 1D and *Materials and Methods*).

In sheared cells ($n = 7$), δ values were about twofold higher than in unsheared cells ($n = 5$, Figure 1C) after 40 min of shear flow and the nuclei of sheared cells moved ~40% of their equivalent radii (Figure 1C). Both nucleus shape (σ)

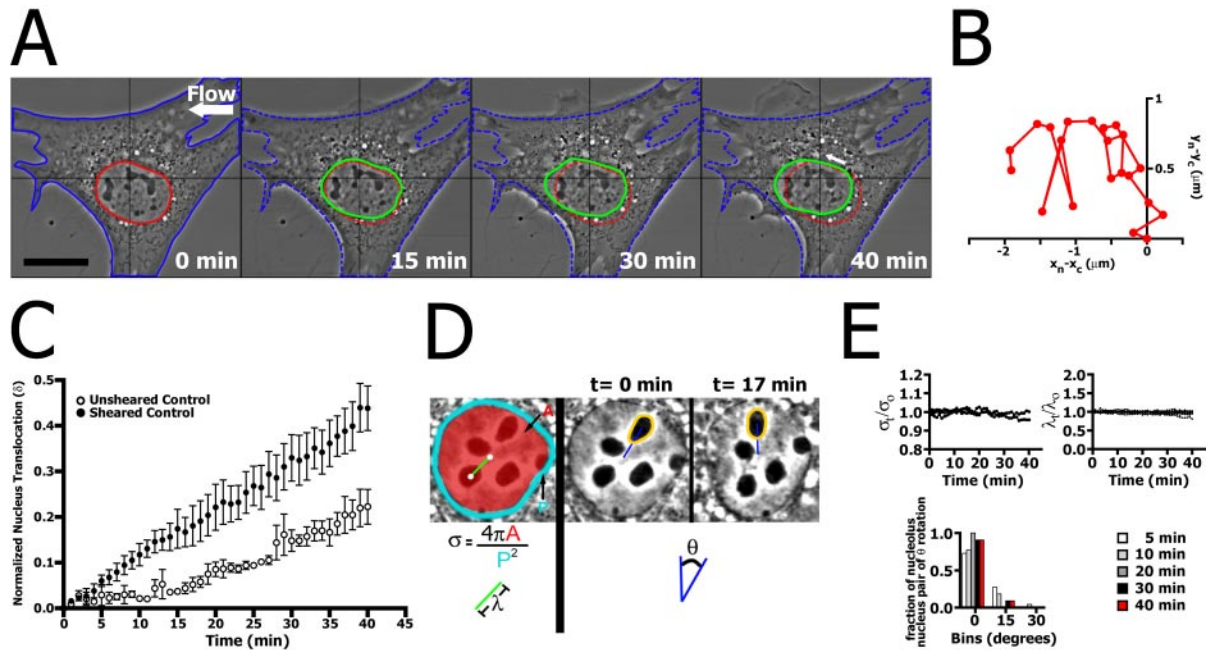


Figure 1. External mechanical shear stress enhances rigid-body movements of the nucleus in Swiss 3T3 fibroblasts. (A) Time-lapse phase contrast sequence of a Swiss 3T3 fibroblast subjected to shear flow for 40 min (shear stress 9.4 dyn/cm²). In the first frame, the solid red circle indicates the initial position and shape of the nucleus. For reference, subsequent dashed red circles mark the initial position of the nucleus. The green circles indicate the instantaneous position and shape of the nucleus. Bar, 20 μ m. (B) Net displacement of the nucleus (corrected for cell displacement) in the sheared fibroblast shown in A, using time-dependent coordinates of the nucleus centroid (x_n, y_n) and the cell centroid (x_c, y_c). (C) Normalized nucleus translocation (δ) of sheared cells (\bullet , $n = 7$) and unsheared control cells (\circ , $n = 5$). (D) Schematic for the computation of nucleus shape factor σ (using both the apparent area, A , and perimeter, P , of the nucleus), nucleus-nucleolus interdistance λ , and nucleus rotation θ . Both λ and θ are computed using centroid positions of the nucleus and nucleoli as indicated by white dots (see *Materials and Methods*). (E) Changes in nucleus shape factor σ and nucleus-nucleolus interdistances λ normalized by their respective initial values, σ_0 and λ_0 , and distribution of nucleus rotation (θ) in control sheared fibroblasts ($n = 7$).

and intranuclear organization (λ) remained mostly intact throughout the course of the experiment, i.e., the nucleus of sheared cells showed enhanced movement without changing shape (Figure 1E and Supplementary Movie 1). We denote this type of motion, “rigid-body” motion. At early times, approximately a quarter of nucleus-nucleolus pairs exhibited at least 15° rotation (white and gray bars in Figure 1E). However, such NR ceased after 10 min of shear flow (black and red bars in Figure 1E). Because λ and σ values were constant during rotation, we describe this behavior as concerted nucleus rotation.

F-actin Depolymerization Does Not Affect Significantly Nucleus Motion

To investigate the mechanisms underlying rigid-body nucleus movement, we first examined the contributions of well-known major cytoskeletal structures, i.e., F-actin and MT. F-actin structure was depolymerized within Swiss 3T3 fibroblasts using varying concentrations of LA-B before shear flow (Figure 2A). Immunofluorescence of actin filament structure revealed extensive depolymerization in the lamella region for all tested LA-B concentrations, but F-actin structures around the nucleus were not replaced completely by small actin aggregates until LA-B reached a concentration of 1.6 μ M (Figure 2A). At this concentration, the fibroblasts exhibited typical LA-B-treated morphology (Bershadsky *et al.*, 1995), but the cells were too weakly anchored to the substratum to resist shear flows for an extended period of time. This was also the case for cells treated with 630 nM

LA-B, although the cells were adherent for 25 min of shear flow. All nuclei of sheared cells treated with 630 nM LA-B or less ($n = 10$) exhibited movements similar to control cells (unpublished data). At 315 nM LA-B, cells ($n = 3$) were adherent for at least 40 min and continued to exhibit rigid-body nuclei movements. The plot of δ values showed that translocation of the nucleus was unaffected by LA-B treatment (Figure 2B). Fluorescence microscopy of 315 nM LA-B-treated cells revealed minor F-actin structures near the nuclei, whereas most F-actin was depolymerized in the lamella and perinuclear region (Figure 2A). Thus, F-actin cannot be dismissed entirely as a contributor to the coordinated motion of the nucleus because of minor residual F-actin structures that remains due to the nature of our assay. However, our results suggest that significant F-actin depolymerization does not affect the rigid-body movement in Swiss 3T3 fibroblasts under mechanical stress.

MT Disruption Affects Nucleus Morphology and Eliminates Rigid-Body NR

We next investigated the effect of MT integrity on nucleus motion due to their abundance in cells, especially around the nucleus (Lane and Allan, 1998). Cells were treated with the MT-disrupting agent nocodazole for 30 min before shear ($n = 3$). Cells showed spotted MT staining with no distinct MTOC (Figure 3A), while retaining an intact F-actin network (Figure 3A, inset). Phase contrast microscopy revealed a very ductile nucleus (Figure 3B and Supplementary Movie 6). Time-dependent values of σ and λ were no longer mostly

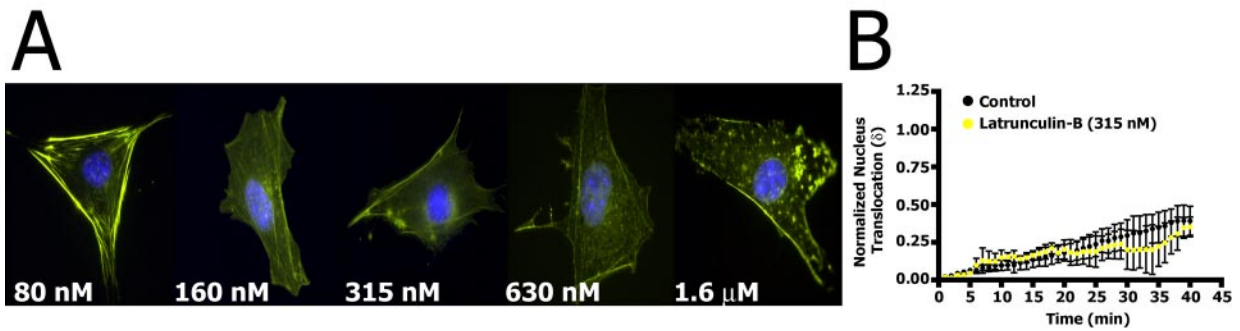


Figure 2. Cell treatment with the F-actin depolymerizing agent latrunculin-B causes no change in the motion of the nucleus. (A) F-actin organization in Swiss 3T3 fibroblasts treated with varying concentrations of F-actin depolymerizing agent, latrunculin-B (LA-B), for 30 min. F-actin and nuclear DNA were visualized using Alexa-488 phalloidin and DAPI, respectively. F-actin depolymerization in the perinuclear region is evident for all tested LA-B concentrations. Significant F-actin depolymerization in the lamella did not occur until 315 nM. Bar, 20 μ m. (B) Normalized nucleus centroid translocation of sheared control cells (black, $n = 7$) and LA-B-treated fibroblasts (315 nM, yellow, $n = 3$).

within 5% of their initial value (Figure 3C). Hence, without an intact MT structure surrounding the nucleus, not only does the rigidity of the nuclear envelope become compromised, but the movements of nucleoli within the nucleus also become independent from each other. The distribution of rotation of nucleus-nucleolus pairs was also wider than in control cells, with some pairs of nucleus-nucleolus rotating as much as 30° from their starting position (Figure 3C). However, because both σ and λ vary dramatically, the rotation can no longer be considered concerted. In the absence of shear, the translocation of the nuclei of nocodazole-treated cells ($n = 3$) was slightly higher than in control cells (Figure 3D). In the presence of shear, the nuclei of nocodazole-treated fibroblasts ($n = 3$) exhibited dramatically increased translocation compared with untreated cells (Figure 3D).

However, as with rotation, such translocation cannot be considered rigid-body motion because of widely varying σ and λ values. In contrast to F-actin depolymerization, MT depolymerization inside Swiss 3T3 fibroblasts causes both the intranuclear region and the nuclear membrane to become compromised, leading to enhanced nonconcerted nucleus movements.

Cdc42 Inactivation Causes Sustained NR

Next, we investigated, through inactivation of individual Rho GTPases, how reorganization, rather than bulk depolymerization, of cytoskeletal structures would affect nucleus motion. Members of the RhoGTPases family, RhoA, Rac1, and Cdc42, have all been shown previously to be involved in the reorganization of both F-actin and MT networks (Nobes

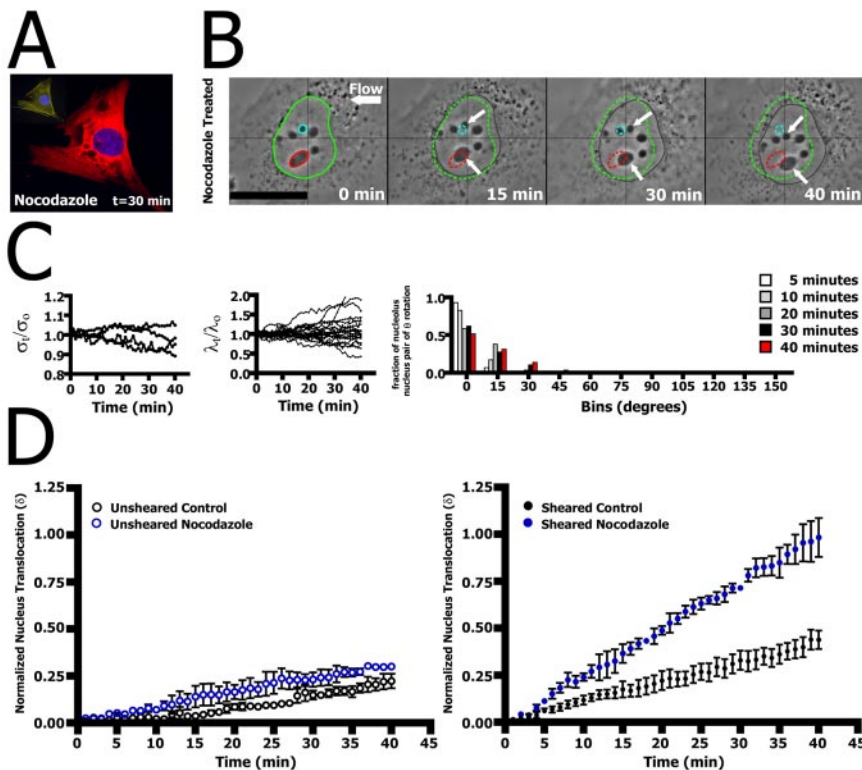


Figure 3. The movement of the nucleus depends on the integrity of microtubules. (A) MT organization in fibroblasts treated for 30 min with 1 μ g/ml nocodazole. Immunofluorescence of MT, nuclear DNA, and F-actin showed completely depolymerized MT structure with intact F-actin structure (inset). (B) Time-lapse phase contrast sequence of sheared fibroblast treated with nocodazole reveals a highly ductile nucleus. Solid and dashed colored circles indicate the initial position of the nucleus (green) and the initial positions of nucleoli (cyan and red); white arrows show the instantaneous location of the nucleoli. Bar, 20 μ m. (C) Changes in nucleus shape factor σ and nucleus-nucleolus interdistances λ , normalized by their respective initial values, σ_0 and λ_0 , and distribution of nucleus rotation θ in nocodazole-treated sheared fibroblasts ($n = 3$). Wider distributions of σ/σ_0 and λ/λ_0 indicate changes in nucleus integrity, as well as nonconcerted movement of the nucleus. (D) Left: nucleus translocation in unsheared control cells ($n = 5$) and nocodazole-treated cells ($n = 3$). Right: nucleus translocation in sheared control cells ($n = 7$) and nocodazole-treated cells ($n = 3$).

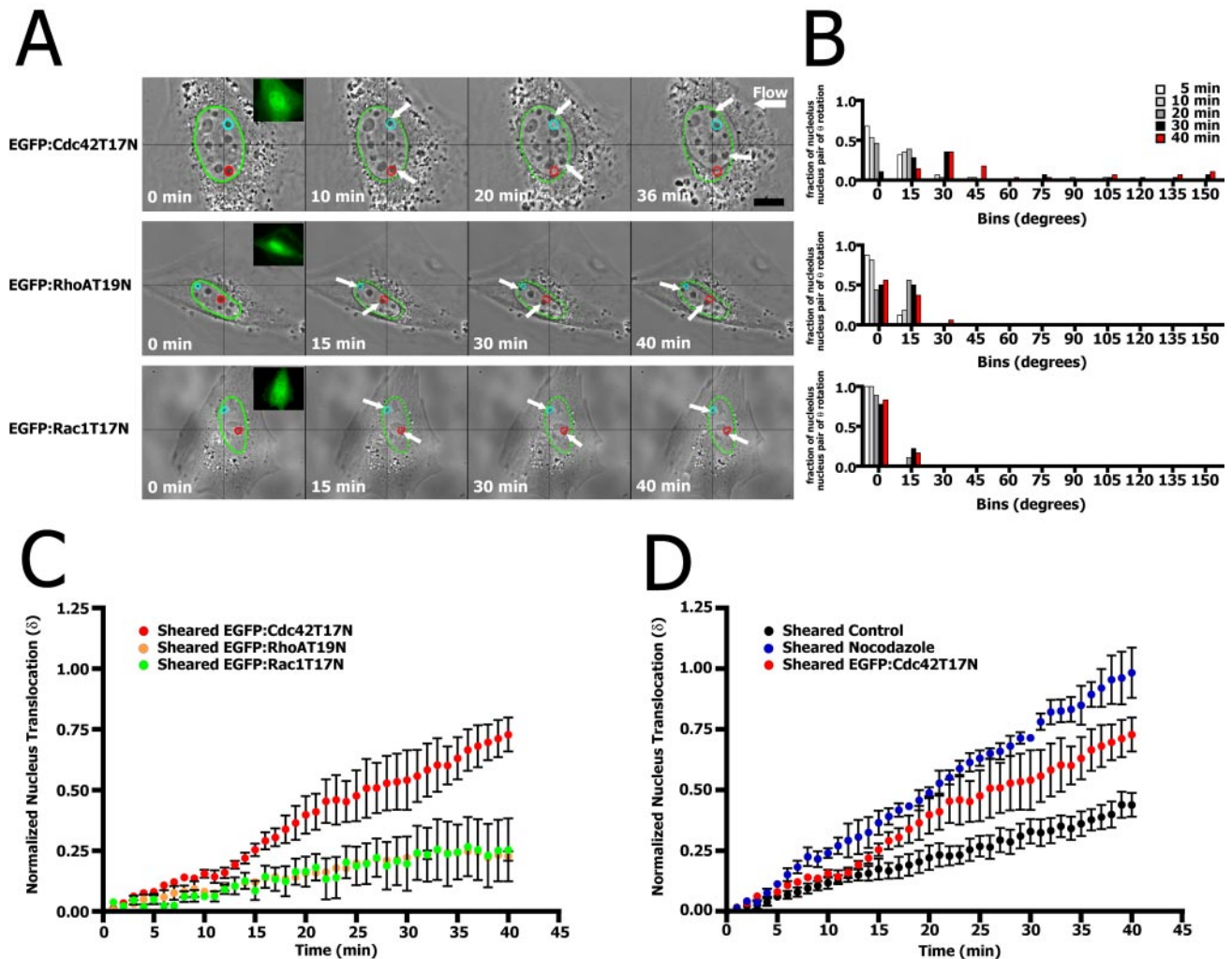


Figure 4. Dominant negative Cdc42 causes sustained nucleus rotation and enhanced nucleus translocation in fibroblasts under shear stress. (A) Time-lapse phase contrast sequence of sheared fibroblasts transfected with either EGFP:Cdc42T17N (first row), EGFP:RhoAT19N (second row), or EGFP:Rac1T17N (third row). EGFP fluorescence indicates that cells are positively transfected (inset). Solid and dashed lines show the initial position and shape of the nucleus (green) and nucleoli (red and cyan); white arrows indicate the instantaneous location of nucleoli. Bar, 20 μ m. (B) Distribution of nucleus rotations in sheared cells transfected with either EGFP:Cdc42T17N (first row, $n = 5$), EGFP:RhoAT19N (second row, $n = 3$), or EGFP:Rac1T17N (third row, $n = 3$). Final rotation distributions are shown in red. (C) Normalized nucleus translocation in sheared cells transfected with either EGFP:Cdc42T17N (red, $n = 5$), EGFP:RhoAT19N (yellow, $n = 3$), or EGFP:Rac1T17N (green, $n = 3$). (D) Comparison of normalized nucleus translocation of sheared control cells (black, $n = 7$), in cells treated with nocodazole (blue, $n = 3$), and cells transfected with EGFP:Cdc42T17N (red, $n = 5$). Translocations of nuclei in EGFP:Cdc42T17N cells is comparable to control nuclei at early times ($t < 15$ min), but becomes greater afterward, moving nearly as much as nocodazole-treated nuclei.

and Hall, 1995, 1999; Bishop and Hall, 2000). Constructs of EGFP-fused RhoGTPases were generated to confirm positive transfection (Figure 4A, inset). Compared with control sheared cells, transfection of either EGFP:Cdc42T17N ($n = 5$), EGFP:RhoAT19N ($n = 3$), or EGFP:Rac1T17N ($n = 3$) into Swiss 3T3 fibroblasts caused minor changes in both σ and λ values (Supplementary Figure 1). But, transfection of EGFP:Cdc42T17N caused the nuclei of sheared fibroblasts to undergo sustained concerted NR (Figures 4B). Initially ($t = 5$ – 10 min), the nuclei of EGFP:Cdc42T17N transfected cells displayed a degree of rotation similar to control cells (Figures 1E and 4B). However, whereas the nucleus of control cells ceased to rotate after 10 min of shear flow, the nuclei of EGFP:Cdc42T17N transfected fibroblasts continued to rotate, with some of the nucleus-nucleolus pairs rotating as much as 10 times more than in control cells (black and red

bars, Figure 4B). Unlike in nocodazole-treated cells, this enhanced rotation was not artificially increased by nucleus deformation because changes in λ and σ were comparable to control fibroblasts (Supplementary Figure 1). The translocation profiles of nuclei in fibroblasts transfected with EGFP:Cdc42T17N were dramatically different from those in control cells (Figures 4D). At early times ($t < 10$ min), δ was comparable to control cells; however, at $t > 10$ min, δ increased sharply and became similar to δ observed in cells treated with nocodazole (Figure 4D). In contrast to transfection of dominant negative Cdc42, transfection of EGFP:Rac1T17N yielded morphometric (λ , σ) and dynamic parameters (θ , δ) that were similar to those found in sheared control cells (Figure 4, B and C). EGFP:RhoAT19N transfection caused a shift in the distribution of nucleus-nucleolus pairs that rotated at early time scales but did not cause any

significant increase in either θ or δ (Figure 4, B and C). Together these results suggest that Cdc42, not RhoA or Rac1, is involved in regulating both rotation and translocation of the nucleus in Swiss 3T3 fibroblasts under mechanical stress.

Shear Flow Promotes MTOC Repositioning in Swiss 3T3 Fibroblasts

We find that under shear flow, changes in either Cdc42 activity or MT integrity significantly affects the motion of the nucleus. Interestingly, Cdc42 and MT also play major roles in cell polarization (Hall, 1998; Johnson, 1999; Palazzo *et al.*, 2001; Small *et al.*, 2002; Fukata *et al.*, 2003; Magdalena *et al.*, 2003b). Structurally, the minus ends of MTs anchor at the MTOC, or the centrosome, which is positioned in close proximity to the nucleus in interphase fibroblasts (Lane and Allan, 1998; Magdalena *et al.*, 2003a). Recently, it has been documented in *C. elegans* that there is a physical link between the centrosome and nucleus via Hook and SUN family proteins (Malone *et al.*, 2003). Therefore, we speculated that our observed shear-induced nucleus motion could be caused by sheared-induced repositioning and polarization of the MTOC in Swiss 3T3 fibroblasts.

To determine changes in cell polarity, we used a MTOC localization assay described previously (Tzima *et al.*, 2003). Through fluorescence microscopy of MT organization and nuclear DNA, we determined the relative positions of the MTOC with respect to the nucleus and the flow direction. By splitting the nucleus into two hemispheres—one in the direction of flow, one in the direction opposite of flow, and noting the location of the MTOC in relation to the demarcation line—the position of the MTOC was used as a marker of cell polarity (white lines and circles in Figure 5A). This standard MTOC localization assay was first carried out in unsheared cells ($n = 75$), for which the distribution of MTOC location was verified to be isotropic, i.e., 50:50 distribution on either side of the demarcation line (Figure 5B). Because the cells were transfected with various EGFP containing constructs, we also transfected the cells with blank EGFP plasmids and verified that the transfection process did not affect the random distribution of MTOC location (unpublished data). The cells were then sheared for 40 min and fixed for subsequent fluorescence microscopy. In sheared control cells ($n = 75$), the MTOC localized predominantly in the flow direction (Figure 5B). These results indicate that shear flow not only enhances nucleus motion, but also induces MTOC repositioning in Swiss 3T3 fibroblasts in the direction of flow.

Cdc42 Inactivation, Not RhoA or Rac1, Inhibits MTOC Polarization in Sheared Fibroblasts

We then investigated if inactivation of RhoGTPases would eliminate shear-induced polarization in Swiss 3T3 fibroblasts. In the absence of shear, control cells and cells transfected with either EGFP:RhoAT19N, EGFP:Rac1T17N, or EGFP:Cdc42T17N preserved an isotropic distribution of the MTOC around the nucleus (Figure 5B). When subject to shear flow, cells transfected with either EGFP:RhoAT19N or EGFP:Rac1T17N continued to exhibit a polarized MTOC distribution similar to control sheared cells (Figure 5B). However, transfection of EGFP:Cdc42T17N abolished shear-induced repositioning of the MTOC in the direction of flow (Figure 5B).

To ensure that MTOC polarization in fibroblasts is indeed regulated by the Cdc42 signaling pathway, we investigated downstream effectors of Cdc42. In MDCK and COS-7 cell lines, Cdc42 forms a complex with partitioning-defective protein, Par6, and mammalian atypical PKC, PKC ζ (Joberty

et al., 2000). Because polarization depends on the complex Cdc42-Par6-PKC ζ in sheared endothelial cells and astrocytes (Etienne-Manneville and Hall, 2001, 2003; Tzima *et al.*, 2003; Wojciak-Stothard and Ridley, 2003), we speculated that Cdc42 mediated MTOC reorientation in Swiss 3T3 fibroblasts through similar interactions with Par6 and PKC ζ .

Swiss 3T3 fibroblasts were transfected with both wild-type and inactive forms of Par6B and PKC ζ , respectively. To test for positive transfection, a blank EGFP vector was transfected along with Par6B and PKC ζ vectors at a 1:10 ratio (Tzima *et al.*, 2003). Cells showing positive transfection of Par6B and PKC ζ vectors displayed green fluorescence similar to cells transfected with EGFP fused RhoGTPases (Figure 5A). Transfections of wild-type Par6B and PKC ζ preserved an even MTOC distribution when the cells were unsheared and a polarized MTOC distribution when the cells were sheared (Figure 5B). Therefore, wild-type Par6B and PKC ζ transfections did not alter the response of cells polarized by shear flow. However, cells transfected with kinase inactive PKC ζ abolished shear-induced MTOC polarization (Figure 5B). The same results were obtained for Δ Nt Par6B (Figure 5B). Together, these results suggest that inactivation of Cdc42, but not of RhoA or Rac1, abrogates sheared-induced MTOC polarization in Swiss 3T3 fibroblasts. Also, even if Cdc42 is active, without normal Par6B or PKC ζ to interact with, the signal cannot be propagated downstream of Cdc42 to promote MTOC repositioning in sheared cells.

DISCUSSION

Our results show that mild mechanical shear stress induces MTOC polarization in Swiss 3T3 fibroblasts, a process mediated by Cdc42 through its interactions with Par6 and PKC ζ . Shear-induced MTOC polarization is accompanied by the enhanced movement of the nearby nucleus, which is also regulated by Cdc42, and controlled by MT integrity. Nucleus movement and MTOC positioning are regulated by neither RhoA and Rac1, nor F-actin structure. These results suggest that MTOC positioning and nucleus movement are intimately connected and parts of the same signaling Cdc42/MT pathway.

Nucleus Movement Is Mediated by Nonsteric Interactions between Microtubules and the Nuclear Envelope

In the absence of shear flow, the movement of the nucleus is relatively constrained in Swiss 3T3 fibroblasts. Nucleus motion can be restricted by either steric or direct interactions between cytoplasmic structures and the nuclear envelope. Steric interactions are caused by friction of the nucleus moving in the viscous cytoskeleton (Kole *et al.*, 2004). MT and actin filaments form a highly viscoelastic network that could, a priori, prevent free motion of the nucleus in the cytoplasm because its mean mesh size (~ 50 nm) is much smaller than the size of the nucleus (~ 25 – 40 μ m; Luby-Phelps *et al.*, 1987; Heidemann and Wirtz, 2004). The main cytoskeletal contributor to cytoplasmic viscoelasticity is F-actin, not MT. Indeed, depolymerization of F-actin greatly reduces the viscosity and elasticity of the cytoplasm of Swiss 3T3 fibroblasts, whereas MT depolymerization leaves cytoplasmic viscoelasticity unchanged (Yamada *et al.*, 2000; Tseng *et al.*, 2002). However, our results reveal that F-actin does not affect the movements of the nucleus.

This suggests that the motion of nucleus cannot be considered merely as passive diffusion through the cytoplasm. If we assumed that nucleus migration consisted of random Brownian motion in a viscous cytoplasmic environment,

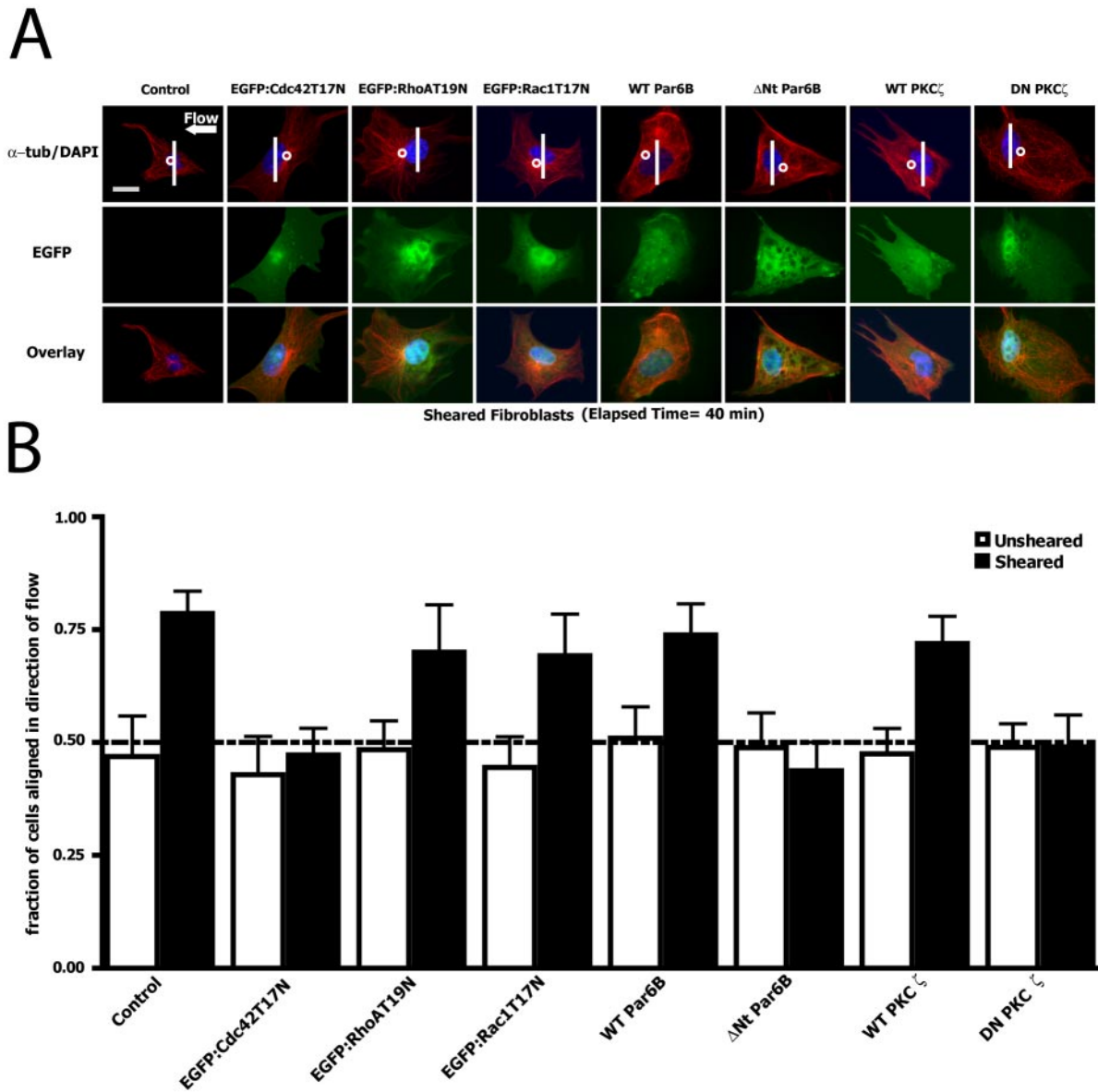


Figure 5. The MTOC of sheared fibroblasts is polarized and its location with respect to the nucleus is controlled by Cdc42. (A) MTOC location in Swiss 3T3 fibroblasts with respect to the nucleus and the shear flow direction. Cells were either transfected with EGFP-tagged constructs (EGFP:Cdc42T17N, EGFP:RhoA19N, EGFP:Rac1T17N) or a combination of protein plasmid (WT Par6B, Δ Nt Par6B, WT PKC ζ , DN PKC ζ) and blank EGFP vector. Proteins were given 24 h to express and positive-transfected fibroblasts exhibited green fluorescence. Fibroblasts were subjected to 40 min of shear flow ($\tau_w = 9.4$ dyn/cm²) and then fixed and stained for MT and nuclear DNA using α -tubulin/Alexa568 and DAPI, respectively. The nucleus was divided into two zones, and MTOC location was determined based on this separation. Bar, 20 μ m. (B) MTOC polarization in fibroblasts is controlled by Cdc42, not RhoA or Rac1. Shear-induced MTOC polarization is inhibited by Cdc42 inactivation and is unaffected by RhoA and Rac1 inactivation. Transfection of EGFP:Cdc42T17N abrogates shear-induced MTOC polarization in Swiss 3T3 fibroblasts. Transfections of EGFP:RhoA19N and EGFP:Rac1T17N did not alter distribution of MTOC location from unsheared transfected cells. Dominant negative/kinase inactive Par6/PKC ζ transfection abolished MTOC polarization, similar to fibroblasts transfected with EGFP:Cdc42T17N. Transfection of wild-type Par6/PKC ζ did not alter shear-induced polarization in the cells ($n = 75$ for all conditions).

using both the recently measured viscosity of the perinuclear region of Swiss 3T3 fibroblast (Tseng *et al.*, 2002) and diffusion theory, we would find that the nucleus migrates ~ 0.5 μ m in 40 min. This distance is much smaller than observed here, even in unsheared cells. Therefore, the viscosity of cytoplasm, primarily set by the F-actin network (Kole *et al.*, 2004), does not limit the rate of migration of the interphase nucleus in fibroblasts. This suggests that nucleus motion is not controlled by steric

interactions but by direct interactions between the nucleus and cytoplasmic structures. Microtubules, which radiate from the MTOC and form a basket of filaments around the interphase nucleus, appear to regulate nucleus movements not by sterically "caging" the nucleus, but by mediating direct interactions with the nucleus (Szabo *et al.*, 2004) and generating supplemental forces that drive the translocation of the nucleus within the cytoplasm (see more below).

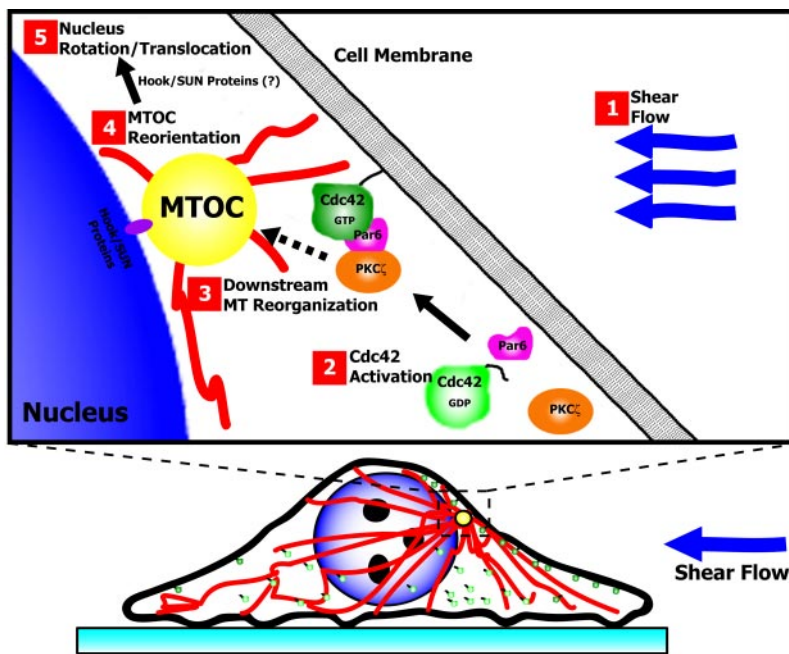


Figure 6. Proposed model for molecular regulation of nucleus movement and MTOC repositioning in Swiss 3T3 fibroblasts under mechanical shear. Shear flow (1) activates Cdc42, which then complexes as Cdc42-GTP to Par6 and PKC ζ (2). Subsequent downstream MT reorganization due to Cdc42/Par6/PKC ζ complex (3) results in MTOC reorientation toward the direction of flow inside Swiss 3T3 fibroblast (4). A physical link between the nucleus and the MTOC, possibly via Hook/SUN family proteins, causes the observed translocation and rotation of the nucleus (5).

MTOC Repositioning and Nucleus Movement Are Mediated by Cdc42

Inactivation of the major actin-cytoskeleton regulators RhoA and Rac1 causes no change in the translocation of the nucleus and MTOC positioning. Nevertheless, RhoA inactivation does increase the number of rotating nucleus-nucleolus pairs, but not the magnitude of rotation, which maybe caused by downstream effectors of RhoA, such as transcription factors and pathways (Bishop and Hall, 2000). The independence of NR on RhoA activity is not entirely surprising as recent work links the Cdc42/Par6/PKC ζ complex to the regulated degradation of RhoA during dynamic movements of the plasma membrane (Wang *et al.*, 2003); moreover, MT polarization has previously been shown to be independent of Rho-dependent contractility in other mammalian cells (Omelchenko *et al.*, 2002). The role of Cdc42 in controlling MTOC positioning in Swiss 3T3 fibroblasts concurs with results previously obtained in the nematode *C. elegans* (Cuenca *et al.*, 2003), astrocytes (Etienne-Manneville and Hall, 2001, 2003), and bovine aortic endothelial cells (BAEC; Tzima *et al.*, 2003). Our results, however, seemingly conflict with those obtained by Wojciak-Stothard and Ridley (2003), who showed that MTOC polarization in human umbilical vein endothelial cells (HUVEC) is mediated by Rho and Rac, not Cdc42. This suggests that the mechanism of polarization is cell-type dependent and that Cdc42 in endothelial cells may not be molecularly linked to the Par6-PKC ζ complex (Wojciak-Stothard and Ridley, 2003). Such differences suggest that the molecules involved in MTOC polarization are cell specific, thereby requiring further investigation into the complexity of polarization in eukaryotic cells.

Our results suggest that nucleus motion is driven by Cdc42-mediated MTOC polarization and is dependent on the integrity of the MT network. The nuclei in control cells and in cells transfected with EGP:Rac1T17N or EGP:RhoAT19N ceased to rotate after a short time, but the nuclei of cells transfected with EGP:Cdc42T17N continue to rotate. We speculate that, under mechanical stress, EGP:Cdc42T17N-expressing cells continuously try to polarize without intracellular orientation cue from Cdc42. This con-

clusion is drawn from noting that Cdc42 inactivation not only causes the loss of specific distribution of MTOC location, but also causes enhanced nucleus rotation and nucleus translocation.

Model of MTOC Repositioning Induced Nucleus Movement

On the basis of our results, we propose the following model of coupled MTOC repositioning and nucleus movement in Swiss 3T3 fibroblasts under shear flow (Figure 6). Enhanced nucleus translocation and rotation at early times during shear suggest that the cell plasma membrane “senses” the shear flow (1 in Figure 6) because of an asymmetry caused by Cdc42 activation (2 in Figure 6) mainly on the plasma membrane that faces the shear flow initially (dark vs. light green in whole cell of Figure 6). Such asymmetry in the cell propagates as only activated Cdc42 binds Par6 (Joberty *et al.*, 2000; Garrard *et al.*, 2003). Upon binding with Par6 and PKC ζ , Cdc42/Par6/PKC ζ complex causes downstream MT reorganization (Joberty *et al.*, 2000; Etienne-Manneville and Hall, 2001; Tzima *et al.*, 2003) and subsequent repositioning of the MTOC in the direction of flow (3 and 4 in Figure 6). MTOC repositioning causes NR and translocation through direct interactions between the MTOC and the nucleus (5 in Figure 6) as argued above. These interactions could involve Hook and SUN family proteins as recent work has shown that in *C. elegans*, ZYG-12, a member of the Hook family of cytoskeletal link proteins, couples the MTOC to the nuclear envelope in a proposed two-step process involving both SUN-1 protein and dynein (Malone *et al.*, 2003). hHK3 and Sun2, homologues of ZYG-12 and SUN-1, respectively, have been recently documented inside mammalian cells (Walenta *et al.*, 2001; Hodzic *et al.*, 2004), making it possible that mammalian cells have a similar two-step process. In a first step, the MTOC is brought in proximity to the nucleus via translocation of dynein, bound to the surface of the nucleus via ZYG-12, on microtubules extending from the MTOC (Malone *et al.*, 2003). During the second step, the MTOC becomes anchored to the nucleus via ZYG-12/ZYG-12 and ZYG-12/SUN-1 binding (Malone *et al.*, 2003). Our results

suggest that the coupled movement of the MTOC and the nucleus in Swiss 3T3 fibroblasts could result from a combination of these two steps.

In the absence of shear flow, growing evidence suggest that the MTOC is attached to the nucleus membrane via the mechanism described in step two (Walenta *et al.*, 2001; Malone *et al.*, 2003; Hodzic *et al.*, 2004). Such steady coupling cannot be maintained during shear-induced MTOC repositioning because it is not only inefficient to drag the nucleus during repositioning, but also extraneous because the MTOC has already been shown to be also responsible for movement of the Golgi apparatus during repositioning (Allan *et al.*, 2002). Instead, our results suggest that upon shear stimulus, nucleus rotation and translocation are caused by dynamic attachment/detachment of the MTOC to/from the nuclear membrane via dynein and Hook/SUN proteins. Such "hopping" of the MTOC would cause nucleus rotation at early times during MTOC reorientation. After reorientation is complete, the MTOC is once again attached to the nucleus membrane, and only translocation would occur. The behavior exhibited by sheared control, EGFP:RhoAT19N-transfected and EGFP:Rac1T17N-transfected fibroblasts concur with such proposal. However, to explain increased rotation in EGFP:Cdc42T17N-transfected fibroblasts, we must examine the role of dynein in Malone *et al.* (2003) proposed step one.

It has been shown that, in NIH 3T3 fibroblasts, function blocking dynein inhibits constitutively active Cdc42-induced MTOC reorientation, which suggests that the activity of dynein could be regulated, either directly or indirectly, by Cdc42 (Palazzo *et al.*, 2001). Therefore, increased nucleus motion in EGFP:Cdc42T17N-transfected fibroblasts could stem from impairment of dynein regulation by Cdc42, which in turn leads to a more permanent attachment of the MTOC and nucleus. Indeed, in mammalian cells, absence of cytoplasmic dynein causes misalignment of organelles, yet the attachment of organelles to MT remains (Harada *et al.*, 1998), indicating other linker proteins exists (Walenta *et al.*, 2001). If the process of dynamic MTOC attachment/detachment from the nuclear membrane is impaired, the MTOC would then be forced to drag the nucleus along as it continuously repositions itself without orientation cue. Indeed, this is what we observed in EGFP:Cdc42T17N-transfected cells, where the nuclei exhibits enhanced translocation and rotation. Recently, it has been found that dynein regulates coupling of the centrosome to the nucleus in migrating mouse neuronal cells (Tanaka *et al.*, 2004). The data reported here suggest that MTOC and nucleus movements are intimately connected and further investigation in mammalian cells is clearly necessary to better understand the coupled movement of the MTOC and the nucleus.

ACKNOWLEDGMENTS

We thank Dr. I. Macara (University of Virginia) for his generous gift of PKC ζ and Par6B plasmids and Dr. J. Lippincott-Schwartz for careful editing of our manuscript. This work was funded by the National Science Foundation (NIRT CTS0210718) and National Aeronautical and Space Administration (NAG9-1563) (to D. Wirtz and Y. Tseng). J. S. Lee was supported by a National Aeronautics and Space Administration training grant (NNG04G054H).

REFERENCES

- Abney, J. R., Cutler, B., Fillbach, M. L., Axelrod, D., and Scalettar, B. A. (1997). Chromatin dynamics in interphase nuclei and its implications for nuclear structure. *J. Cell Biol.* 137, 1459–1468.
- Allan, V. J., Thompson, H. M., and McNiven, M. A. (2002). Motoring around the Golgi. *Nat. Cell Biol.* 4, E236–E242.
- Bandyopadhyay, G., Standaert, M. L., Kikkawa, U., Ono, Y., Moscat, J., and Farese, R. V. (1999). Effects of transiently expressed atypical (zeta, lambda), conventional (alpha, beta) and novel (delta, epsilon) PKC isoforms on insulin-stimulated translocation of epitope-tagged GLUT4 glucose transporters in rat adipocytes: specific interchangeable effects of protein kinases C-zeta and C-lambda. *Biochem. J.* 337(Pt 3), 461–470.
- Bandyopadhyay, G., Standaert, M. L., Zhao, L., Yu, B., Avignon, A., Galloway, L., Karnam, P., Moscat, J., and Farese, R. V. (1997). Activation of PKC (alpha, beta, and zeta) by insulin in 3T3/L1 cells. Transfection studies suggest a role for PKC-zeta in glucose transport. *J. Biol. Chem.* 272, 2551–2558.
- Bershady, A. D., Gluck, U., Denisenko, O. N., Sklyarova, T. V., Spector, I., and Ben-Ze'ev, A. (1995). The state of actin assembly regulates actin and vinculin expression by a feedback loop. *J. Cell Sci.* 108(Pt 3), 1183–1193.
- Bishop, A. L., and Hall, A. (2000). Rho GTPases and their effector proteins. *Biochem. J.* 348, 241–255.
- Cerda, M. C., Berrios, S., Fernandez-Donoso, R., Garagna, S., and Redi, C. (1999). Organisation of complex nuclear domains in somatic mouse cells. *Biol. Cell* 91, 55–65.
- Cerione, R. A. (2004). Cdc42, new roads to travel. *Trends Cell Biol.* 14, 127–132.
- Cuenca, A. A., Schetter, A., Aceto, D., Kempfues, K., and Seydoux, G. (2003). Polarization of the *C. elegans* zygote proceeds via distinct establishment and maintenance phases. *Development* 130, 1255–1265.
- Etienne-Manneville, S. (2004). Cdc42—the centre of polarity. *J. Cell Sci.* 117, 1291–1300.
- Etienne-Manneville, S., and Hall, A. (2001). Integrin-mediated activation of Cdc42 controls cell polarity in migrating astrocytes through PKCzeta. *Cell* 106, 489–498.
- Etienne-Manneville, S., and Hall, A. (2003). Cdc42 regulates GSK-3beta and adenomatous polyposis coli to control cell polarity. *Nature* 421, 753–756.
- Fukata, M., Nakagawa, M., and Kaibuchi, K. (2003). Roles of Rho-family GTPases in cell polarisation and directional migration. *Curr. Opin. Cell Biol.* 15, 590–597.
- Fukata, M., Watanabe, T., Noritake, J., Nakagawa, M., Yamaga, M., Kuroda, S., Matsuura, Y., Iwamatsu, A., Perez, F., and Kaibuchi, K. (2002). Rac1 and Cdc42 capture microtubules through IQGAP1 and CLIP-170. *Cell* 109, 873–885.
- Garrard, S. M., Capaldo, C. T., Gao, L., Rosen, M. K., Macara, I. G., and Tomchick, D. R. (2003). Structure of Cdc42 in a complex with the GTPase-binding domain of the cell polarity protein, Par6. *EMBO J.* 22, 1125–1133.
- Goldstein, A. S., and DiMilla, P. A. (2002). Effect of adsorbed fibronectin concentration on cell adhesion and deformation under shear on hydrophobic surfaces. *J. Biomed. Mater. Res.* 59, 665–675.
- Hagan, I., and Yanagida, M. (1997). Evidence for cell cycle-specific, spindle pole body-mediated, nuclear positioning in the fission yeast *Schizosaccharomyces pombe*. *J. Cell Sci.* 110, 1851–1866.
- Hall, A. (1998). Rho GTPases and the actin cytoskeleton. *Science* 279, 509–514.
- Harada, A., Takei, Y., Kanai, Y., Tanaka, Y., Nonaka, S., and Hirokawa, N. (1998). Golgi vesiculation and lysosome dispersion in cells lacking cytoplasmic dynein. *J. Cell Biol.* 141, 51–59.
- Harwood, A., and Braga, V. M. (2003). Cdc42 & GSK-3, signals at the crossroads. *Nat. Cell Biol.* 5, 275–277.
- Heidemann, S. R., and Wirtz, D. (2004). Towards a regional approach to cell mechanics. *Trends Cell Biol.* 14, 160–166.
- Hodzic, D. M., Yeater, D. B., Bengtsson, L., Otto, H., and Stahl, P. D. (2004). Sun2 is a novel mammalian inner nuclear membrane protein. *J. Biol. Chem.* 279, 25805–25812.
- Hollenbeck, P. (2001). Cytoskeleton: microtubules get the signal. *Curr. Biol.* 11, R820–R823.
- Joberty, G., Petersen, C., Gao, L., and Macara, I. G. (2000). The cell-polarity protein Par6 links Par3 and atypical PKC to Cdc42. *Nat. Cell Biol.* 2, 531–539.
- Johnson, D. I. (1999). Cdc42, an essential Rho-type GTPase controlling eukaryotic cell polarity. *Microbiol. Mol. Biol. Rev.* 63, 54–105.
- Kole, T. P., Tseng, Y., Huang, L., Katz, J. L., and Wirtz, D. (2004). Rho kinase regulates the intracellular micromechanical response of adherent cells to rho activation. *Mol. Biol. Cell* 15, 3475–3484.
- Lane, J., and Allan, V. (1998). Microtubule-based membrane movement. *Biochim. Biophys. Acta* 1376, 27–55.
- Luby-Phelps, K., Castle, P. E., Taylor, D. L., and Lanni, F. (1987). Hindered diffusion of inert tracer particles in the cytoplasm of mouse 3T3 cells. *Proc. Natl. Acad. Sci. USA* 84, 4910–4913.

- Magdalena, J., Millard, T. H., Etienne-Manneville, S., Launay, S., Warwick, H. K., and Machesky, L. M. (2003a). Involvement of the Arp2/3 complex and Scar2 in Golgi polarity in scratch wound models. *Mol. Biol. Cell* *14*, 670–684.
- Magdalena, J., Millard, T. H., and Machesky, L. M. (2003b). Microtubule involvement in NIH 3T3 Golgi and MTOC polarity establishment. *J. Cell Sci.* *116*, 743–756.
- Malone, C. J., Misner, L., Le Bot, N., Tsai, M. C., Campbell, J. M., Ahringer, J., and White, J. G. (2003). The *C. elegans* hook protein, ZYG-12, mediates the essential attachment between the centrosome and nucleus. *Cell* *115*, 825–836.
- Morris, N. R. (2000). Nuclear migration. From fungi to the mammalian brain. *J. Cell Biol.* *148*, 1097–1101.
- Morris, N. R., Efimov, V. P., and Xiang, X. (1998). Nuclear migration, nucleokinesis and lissencephaly. *Trends Cell Biol.* *8*, 467–470.
- Nobes, C. D., and Hall, A. (1995). Rho, rac, and cdc42 GTPases regulate the assembly of multimolecular focal complexes associated with actin stress fibers, lamellipodia, and filopodia. *Cell* *81*, 53–62.
- Nobes, C. D., and Hall, A. (1999). Rho GTPases control polarity, protrusion, and adhesion during cell movement. *J. Cell Biol.* *144*, 1235–1244.
- Omelchenko, T., Vasiliev, J. M., Gelfand, I. M., Feder, H. H., and Bonder, E. M. (2002). Mechanisms of polarization of the shape of fibroblasts and epitheliocytes: separation of the roles of microtubules and Rho-dependent actin-myosin contractility. *Proc. Natl. Acad. Sci. USA* *99*, 10452–10457.
- Paddock, S. W., and Albrecht-Buehler, G. (1986). Distribution of microfilament bundles during rotation of the nucleus in 3T3 cells treated with monensin. *Exp. Cell Res.* *163*, 525–538.
- Paddock, S. W., and Albrecht-Buehler, G. (1988). Rigidity of the nucleus during nuclear rotation in 3T3 cells. *Exp. Cell Res.* *175*, 409–413.
- Palazzo, A. F., Joseph, H. L., Chen, Y. J., Dujardin, D. L., Alberts, A. S., Pfister, K. K., Vallee, R. B., and Gundersen, G. G. (2001). Cdc42, dynein, and dynactin regulate MTOC reorientation independent of Rho-regulated microtubule stabilization. *Curr. Biol.* *11*, 1536–1541.
- Pellettieri, J., and Seydoux, G. (2002). Anterior-posterior polarity in *C. elegans* and *Drosophila*—PARallels and differences. *Science* *298*, 1946–1950.
- Reinsch, S., and Gonczy, P. (1998). Mechanisms of nuclear positioning. *J. Cell Sci.* *111*(Pt 16), 2283–2295.
- Small, J. V., Geiger, B., Kaverina, I., and Bershadsky, A. (2002). How do microtubules guide migrating cells? *Nat. Rev. Mol. Cell Biol.* *3*, 957–964.
- Szabo, B., Kornyei, Z., Zach, J., Selmeczi, D., Csucs, G., Czirik, A., and Vicsek, T. (2004). Auto-reverse nuclear migration in bipolar mammalian cells on micropatterned surfaces. *Cell Motil. Cytoskeleton* *59*, 38–49.
- Tanaka, T., Serneo, F. F., Higgins, C., Gambello, M. J., Wynshaw-Boris, A., and Gleeson, J. G. (2004). Lis1 and doublecortin function with dynein to mediate coupling of the nucleus to the centrosome in neuronal migration. *J. Cell Biol.* *165*, 709–721.
- Tseng, Y., Kole, T. P., and Wirtz, D. (2002). Micromechanical mapping of live cells by multiple-particle-tracking microrheology. *Biophys. J.* *83*, 3162–3176.
- Tseng, Y., Lee, J. S., Kole, T. P., Jiang, I., and Wirtz, D. (2004). Micro-organization and visco-elasticity of the interphase nucleus revealed by particle nanotracking. *J. Cell Sci.* *117*, 2159–2167.
- Tsou, M. F., Ku, W., Hayashi, A., and Rose, L. S. (2003). PAR-dependent and geometry-dependent mechanisms of spindle positioning. *J. Cell Biol.* *160*, 845–855.
- Tzima, E., Del Pozo, M. A., Kioussis, W. B., Mohamed, S. A., Li, S., Chien, S., and Schwartz, M. A. (2002). Activation of Rac1 by shear stress in endothelial cells mediates both cytoskeletal reorganization and effects on gene expression. *EMBO J.* *21*, 6791–6800.
- Tzima, E., Kioussis, W. B., del Pozo, M. A., and Schwartz, M. A. (2003). Localized cdc42 activation, detected using a novel assay, mediates microtubule organizing center positioning in endothelial cells in response to fluid shear stress. *J. Biol. Chem.* *278*, 31020–31023.
- Walenta, J. H., Didier, A. J., Liu, X., and Kramer, H. (2001). The Golgi-associated hook3 protein is a member of a novel family of microtubule-binding proteins. *J. Cell Biol.* *152*, 923–934.
- Wang, H. R., Zhang, Y., Ozdamar, B., Ogunjimi, A. A., Alexandrova, E., Thomsen, G. H., and Wrana, J. L. (2003). Regulation of cell polarity and protrusion formation by targeting RhoA for degradation. *Science* *302*, 1775–1779.
- Wojciak-Stothard, B., and Ridley, A. J. (2003). Shear stress-induced endothelial cell polarization is mediated by Rho and Rac but not Cdc42 or PI 3-kinases. *J. Cell Biol.* *161*, 429–439.
- Yamada, S., Wirtz, D., and Kuo, S. C. (2000). Mechanics of living cells measured by laser tracking microrheology. *Biophys. J.* *78*, 1736–1747.